Static and Dynamic Characteristics of McKibben Pneumatic Artificial Muscles

Ching-Ping Chou and Blake Hannaford

Department of Electrical Engineering, FT-10, University of Washington, Seattle, Washington 98195

Abstract: This paper reports mechanical testing and modeling results for the McKibben artificial muscle pneumatic actuator. This device first developed in the 1950's, contains an expanding tube surrounded by braided cords. We report static and dynamic length-tension testing results and derive a linearized model of these properties for three different models. The results are briefly compared with human muscle properties to evaluate the suitability of McKibben actuators for human muscle emulation in biologically based robot arms.

Introduction

The McKibben pneumatic artificial muscles were developed in artificial limb research in the 1950s and 1960s (Schulte 1961, Gavrilovic and Maric 1969). They have recently been commercialized by the Bridgestone Rubber Company of Japan for robotic applications (Inoue 1988), and re-engineered by Prof. Jack Winters for construction of biomechanically realistic skeletal models. McKibben muscles consist of an internal bladder surrounded by a braided mesh shell (with flexible yet non-extensible threads) that is attached at either end to fittings or to some tendon-like structure. When the internal bladder is pressurized, the high pressure gas pushes against its inner surface and against the external shell, and tends to increase its volume. Due to the non-extensibility (or very high longitudinal stiffness) of the threads in the braided mesh shell, the actuator shortens according to its volume increase and/or produces tension if it is coupled to a mechanical load. This physical configuration causes McKibben muscles to have variable-stiffness spring-like characteristics, non-linear passive elasticity, physical flexibility, and very light weight compare to other kinds of artificial actuators (Hannaford and Winters 1990).

The relationships between tension, length, velocity, and activation are the major characteristics of actuators which vary greatly from type to type. Human skeletal muscle also has its own particular characteristics: the convex shape active tension-length relationship (Gordon et al. 1966), the non-linear passive tension-length relationship, the hyperbolic tension-velocity relationship (Hill 1938), and each of above also is a function of activation level (McMahon 1984, Winters 1990, Zahalak 1990). In order to show the similarity (or not) to biological muscles, three types of McKibben muscles, two designed and made by Dr. Winters and one manufactured by Bridgestone, were tested.

In this article, 1) an idealized static physical model of McKibben muscles will be analyzed with a simple theoretical approach, 2) a series of quasi-static and dynamic experiments will be described using a dynamic testing machine, which show a velocity independent tension-length hysteresis, 3) a simplified static model will be described based on both experimental data and theoretical approach, and 4) the quasi-static and dynamic characteristics will be analyzed.

Finally, the actuators will be compared to biological muscles. In general, the McKibben artificial muscle is much more similar to biological muscles than other kinds of artificial actuators.

Static physical model of McKibben muscles

McKibben muscle is an actuator which converts pneumatic (or hydraulic) energy into mechanical form by transferring the pressure applied on the inner surface of its bladder into the shortening tension. In order to find the tension as a function of pressure and actuator length, without considering the detailed geometric structure, a theoretic approach from the view of energy conservation is described as following.

The input work (W_{in}) is done in McKibben muscle when gas pushes the inner surface of the bladder, which is:

$$dW_{in} = \int_{S_i} (P - P_o)\, d\mathbf{l}_\mathbf{i} \cdot d\mathbf{s}_\mathbf{i} = (P - P_o) \int_{S_i} d\mathbf{l}_\mathbf{i} \cdot d\mathbf{s}_\mathbf{i} = P' dV \quad (1)$$

where P is absolute internal gas pressure, P_o, environment pressure (1 atm), P', relative pressure $(P - P_o)$, S_i, total inner surface, $d\mathbf{s}_\mathbf{i}$, area vector, $d\mathbf{l}_\mathbf{i}$, inner surface displacement, and dV, volume change. The output work (W_{out}) is done when the actuator shortens associated with the volume changes, which is:

$$dW_{out} = -F dL \quad (2)$$

where F is axial tension, and dL is axial displacement. From the view of energy conservation, the input work should equal the output work if a system is lossless and without energy storage. Assume the actuator is in this ideal condition. We can then use the "virtual work" argument:

$$dW_{out} = dW_{in}, \quad (3)$$

thus, from equ. 1 and equ. 2,

This research was conducted with the support the Office of Naval Research (Grant no N00014-92-J-1401).

$$-FdL = P'dV, \tag{4a}$$

$$F = -P'\frac{dV}{dL}. \tag{4b}$$

To estimate dV/dL, the middle portion of the actuator is modeled as a perfect cylinder (Fig.1), where L is the length of the cylinder, θ, the angle between a braided thread and the cylinder long axis, D, the diameter of the cylinder, n, number of turns of a thread, and b, the thread length. L and D can be expressed as functions of θ with constant parameters n and b,

$$L = b\cos\theta, \tag{5}$$

$$D = \frac{b\sin\theta}{n\pi}. \tag{6}$$

The volume of the cylinder is,

$$V = \frac{1}{4}\pi D^2 L = \frac{b^3}{4\pi n^2}\sin^2\theta\cos\theta. \tag{7}$$

So, from equ. 4b, F can be expressed as a function of P' and θ,

$$F = -P'\frac{dV}{dL} = -P'\frac{dV/d\theta}{dL/d\theta} = \frac{P'b^2(3\cos^2\theta - 1)}{4\pi n^2}, \tag{8a}$$

which is equivalent to

$$F = \frac{\pi D_o^2 P'}{4}(3\cos^2\theta - 1) \tag{8b}$$

where $D_o = b/n\pi$, is the diameter when θ equals 90°, the form used in Schulte's paper (1961)).

The tension is thus linearly proportional to the pressure, and is a monotonic function of the braid angle. The maximal shortening will be reached when $F = 0$, that is, $\theta = 54.7°$. However, if the thickness (t_k) of the shell and bladder is considered, the relation becomes

$$V = \frac{1}{4}\pi(D - 2t_k)^2 L, \tag{9}$$

by plugging into equ. 4b,

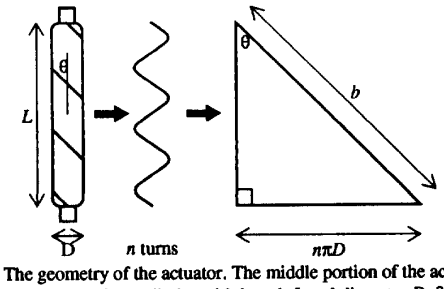

Fig. 1 The geometry of the actuator. The middle portion of the actuator is modeled as a perfect cylinder with length L and diameter D. θ is the angle between a braided thread and the cylinder long axis, n, number of turns of a thread, and b, the thread length. The relationship between the above parameters is illustrated by the triangle.

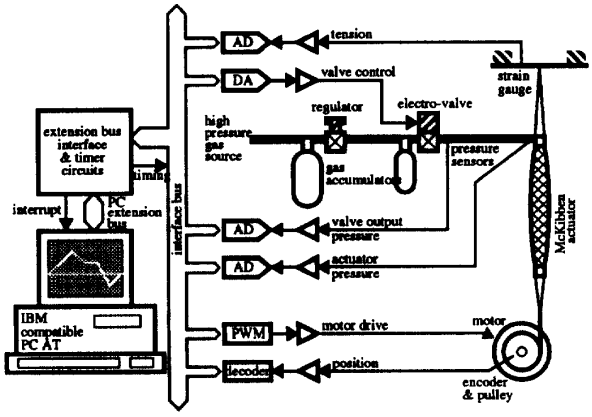

Fig. 2 Block diagram of the dynamic testing machine.

$$F = -P'\frac{dV}{dL} = \frac{\pi D_o^2 P'}{4}(3\cos^2\theta - 1) + \pi P'\left[D_o t_k\left(2\sin\theta - \frac{1}{\sin\theta}\right) - t_k^2\right]. \tag{10}$$

This is more complex than equ. 8b.

Quasi-static and dynamic experiments

For the following experiments, a testing system capable of producing and recording desired patterns of the tension, length, and pressure of the actuator was built (Fig.2).

The hardware includes an IBM compatible personal computer (PC), PC extension bus interface and any necessary digital and analog circuits, pressure sensors (6.8 bar max.), a pressure regulator, a electro-valve (10 bar max.), strain gauge force sensors (100 N max.), a 1/4 horse power DC motor, pulse-width-modulation power amplifier (± 24 A max. current), an optical angular position incremental encoder (1600 steps per revolution), and a testing frame (12"w × 20"h × 8"d) to mount the mechanical parts, sensors, and the actuator.The software includes real time position and force control, data acquisition and user interface.

By utilizing different combinations of the I/O channels and software settings, the system can performs a variety of testing conditions, such as constant pressure testing, isometric testing, isotonic testing, pneumatic circuit testing, or fully dynamic testing, etc. However, only the constant pressure testing is applied in this article.

Since there is no analytical solution to describe biological muscle tension-length-activation relationship, a variety of configurations have been choose to illustrate part of this relationship, such as static tension-length relation under constant activation level (Gordon et al. 1966), isometric to isotonic quick release experiment (Gasser and Hill 1924), isokinetic experiment (Gasser and Hill 1924, Levin and Wyman 1927), isometric tension in response to activation

(Burke et al. 1976, Chou and Hannaford 1992), etc. Notice that the activation is always as an input to muscle mechanics, and either one of the other two quantities (the tension and the length) may be as an input and the other as an output. The pressure of the actuator is analogous to the activation level and will initially be thought of as an input to the actuator, which will be held as constant as possible in these experiments in order to minimize the effects of the pressure dynamics and thus simplify the analysis.

Three types of actuators were tested in quasi-static experiments and one was also tested in dynamic experiments. The first one with nylon shell is 14 cm resting length, and 1.1 cm in diameter at 5 bar no load. The second one with fiberglass shell is 20 cm in length, 0.9 cm in diameter. And the third one, manufactured by Bridgestone, is 14.7 cm in length, 1.5 cm in diameter

In quasi-static experiments, first, the nylon shell actuator was tested. A set of low frequency triangular wave displacements (relative to resting length, L_o = 14 cm) to best cover the linear tension regions corresponding to different pressure levels are selected as the input. The displacements are set to 1 Hz with large operating range (which yields the peak velocity about 0.5 L_o/s).

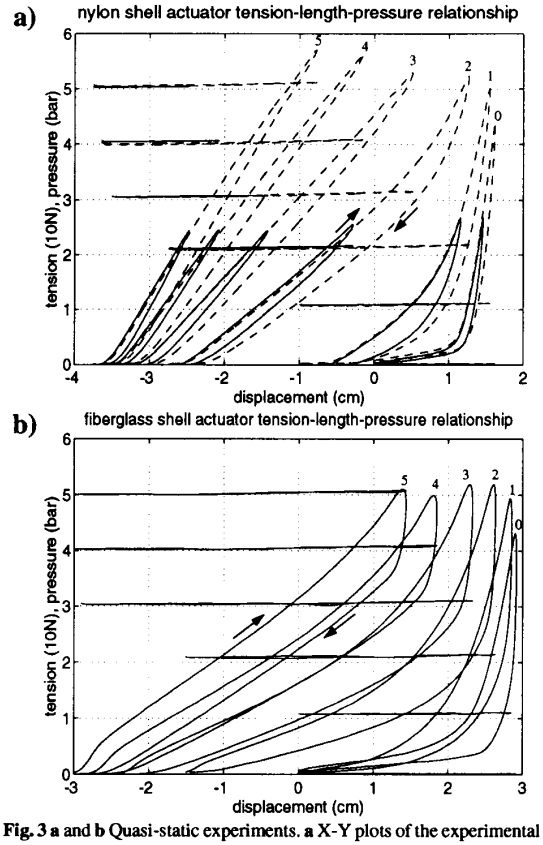

Fig. 3 a and **b** Quasi-static experiments. **a** X-Y plots of the experimental results for the nylon shell actuator. Six pairs of curves are superimposed in the plots: nearly horizontal curves, the measured pressure-length, sloped curves, the tension-length. The hysteresis direction is clockwise. Dashed lines, large range, 1 Hz. Solid lines, small range, 1 Hz. **b** X-Y plot of the experimental results for the fiberglass shell actuator.

The pressure is set by a manual regulator to obtain six desired constant levels (relative 0-5 bar). Due to 1) the volume change of the actuator according to the length change, 2) the gas viscosity in the connection tubing, and 3) the regulator's output hysteresis, the measured pressure will increase when the actuator lengthens and will decrease when it shortens with hysteresis loop. In order to reduce the variation of the pressure, a 10 in^3 (164 cm^3) accumulator is connected to the regulator, and a 3 in^3 (49 cm^3) accumulator is connected directly to the actuator. As a result, the pressure variation was limited to less than 0.1 bar due to the large total capacity of the accumulators, and the pressure hysteresis is almost immeasurable due to the close position (to the actuator) of the second accumulator.

Both the measured pressure and the tension are shown in response to the displacements (Fig.3a, dashed lines). By minimizing the effect of pressure variation, the hysteresis loop of the tension-length relationship is illuminated. The width and height of the loop is about 0.2-0.5 cm and 5-10 N respectively. Two further experiments were made to illustrate more features of the hysteresis.

First, the frequency of the displacement waveforms is reduced to 0.25 Hz, while the operating range remains the same (which yields the peak velocity about 0.125 L_o/s). The result is almost identical to the previous case, which suggests that the tension-length behavior is velocity (low velocity) independent. Second, the frequency is set to 1 Hz, while the operating range is reduced about half (Fig.3a, solid lines). The tension rising paths remain the same (the rising "initial conditions" are the same), but the falling paths are different (The falling "initial conditions" are different due to the smaller operating range). Thus the width and height of the loop are reduced. This indicates the hysteresis is history dependent.

The procedure to obtain Fig.3a was repeated for the fiberglass actuator, and the results in the same format are shown in Fig.3b. Similar tests were performed for the commercially available Bridgestone actuator (Chou and Hannaford 1993). The stiffness, friction, and extensibility are quite different in the above three actuators.

In dynamic experiments, only the first actuator was tested. A set of middle to high frequency sinusoidal displacement waveforms (relative to zero tension length) with small operating range is applied. The pressure is set to relative 5 bar, and remains constant quite well in this condition (due to smaller length change). The frequencies and displacement range are designed to obtain 0.2-8.0 L_o/s peak velocity yet remain in the linear tension-length region. The viscous friction (damping force) if measurable, would be revealed by a hysteresis width which is a mono-

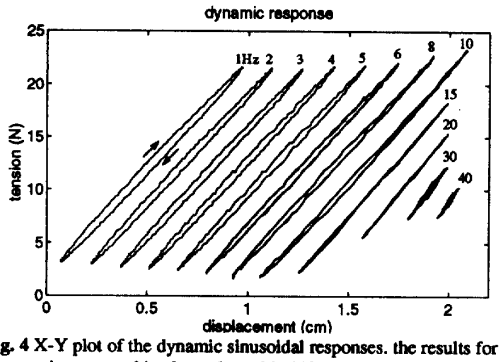

Fig. 4 X-Y plot of the dynamic sinusoidal responses. the results for 12 frequencies are combined together with shifting. Notice the width of the hysteresis is almost unchanged for peak velocity from 0.2 L_o/s (1 Hz) to 2.0 L_o/s (10 Hz). The hysteresis direction is clockwise.

tonic increasing function of the velocity. However, the results show that the width of the tension-displacement loop is very small and almost unchanged, except for a slight decrease at higher frequency (Fig.4).

These results indicate that the velocity-independent hysteresis is most likely to be the Coulomb friction, which dominates the total friction of the actuator. The viscous friction is much smaller than Coulomb friction and thus immeasurable.

An attempt to reduce the Coulomb friction was performed by applying three types of lubricant (including "WD-40 stops squeaks", 10W-40 engine oil, and another kind of small machine oil) on the braided shell and bladder of the nylon actuator. Only 10% of Coulomb friction were reduced by these measures. A special type of lubricant is probably required to reduce the friction of plastic-plastic contacts.

Simplified static model

Excluding the above Coulomb friction, a hypothetical static tension-length relation can be estimated by equ. 10. The actuator can also be considered as a variable-stiffness elastic element, or a "gas spring", where the tension is a function of the pressure and the length. Its stiffness ($K \equiv dF/dL$) is proportional to the pressure, and the stiffness per unit pressure ($K_g \equiv dK/dP'$) approximates a constant within 10 to 14 cm length by simulation (K_g = 0.461 cm, or 4.61 N/cm·bar, with estimating the effective thickness t_k = 0.0762 cm and the diameter D_o = 1.66 cm). So, fortunately, it can be linearized as:

$$F = K_g P' (L - L_{min}) \tag{11}$$

where L_{min} is the theoretically possible minimum length (when $F = 0$).

Consider energy stored by the actuator in its bladder and shell, yielding

$$F = K_g (P' - P_{th}) (L - L_{min}) + K_p (L - L_o) + nl(L) \quad \text{if } P' > P_{th}, \text{ or} \tag{12a}$$

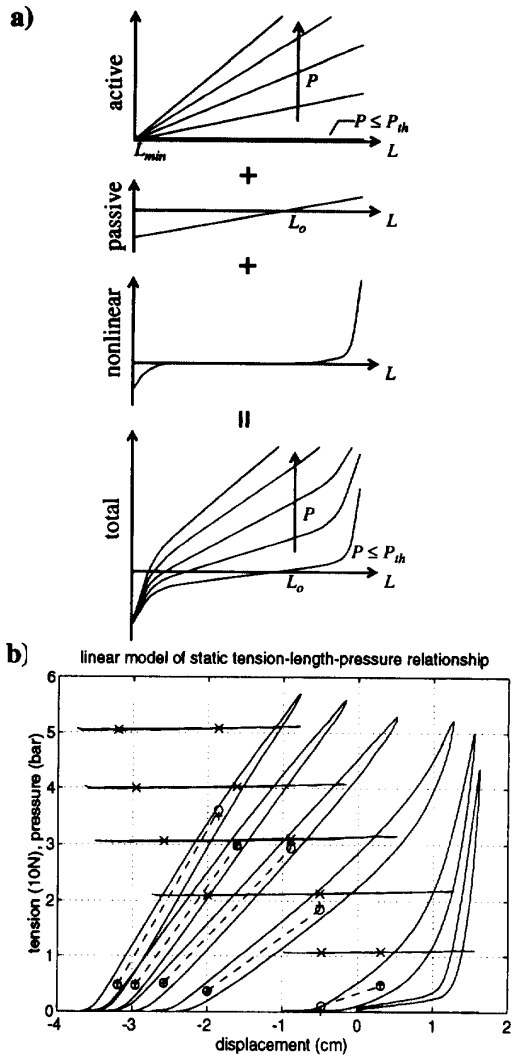

Fig. 5 a and b The static model of the actuator. a the total tension is the summation of the active term, passive term, and non-linear term. b The parameters of the linearized model are optimized with 10 tension-length-pressure sample points from experimental data of Fig. 3a. x, sampled pressure, +, sampled tension, o, simulation tension.

$$F = K_p (L - L_o) + nl(L) \quad \text{if } P' \le P_{th} \tag{12b}$$

where P_{th} is the threshold for the pressure to overcome the radial elasticity of the bladder for expanding, K_p is the linearized equivalent parallel passive elastic constant for the shearing force of the bladder material and shell threads, and $nl(\cdot)$ is the non-linear term due to the non-perfect cylinder while the actuator is at its extreme length (Fig.5a). The first two product terms in equ. 12a can be expressed as

$$F = K_g (P' - P_a) (L - L_{min}) + F_a \tag{13}$$

where $P_a = P_{th} - K_p/K_g$, and $F_a = K_p (L_{min} - L_o)$. To

experimentally estimate these parameters, 10 points of hypothetical static tension-length-pressure pairs are sampled from above quasi-static results and fit into equ. 13 (Fig.5b), thus obtain K_g = 0.466 cm, P_a = 0.062 bar, L_{min} = 9.91 cm, and F_a = -16.0 N. Also, P_{th} and K_p can be estimated by knowing L_o = 14.0 cm, which yields P_{th} = 0.903 bar and K_p = 3.92 N/cm. Notice the K_g is very close to the theoretical value 0.461 cm. The non-linear term only becomes significant when the actuator is extremely short or extremely long, usually this is out of regular operating range, and will not be discussed further.

Quasi-static and dynamic characteristics

It has been shown that there is hysteresis in the tension-length cycle, and that the dominant friction is the frequency insensitive Coulomb friction, which is caused by the contact between the bladder and the shell, between the braided threads and each other, and the shape changing of the bladder. The history dependence makes the friction difficult to predict precisely, especially after the actuator is attached to artificial bones with curving shape. So, for the actuator tested in Fig.3a, it is suggested to add a typical friction value (± 2.5 N, positive for lengthening, negative for shortening) to the hypothetical static equation (equ. 12a or 13 and 12b) if simplicity is necessary.

Summary

We have measured the mechanical characteristics of the McKibben muscles (the actuators), which behaves like a variable-stiffness elastic element with velocity-insensitive friction. The stiffness is mostly dependent on the internal gas pressure, however, in order to produce tension, the pressure must be higher than a threshold to overcome the radial elasticity of the bladder. Also, a piecewise-linear, static model of the McKibben muscle has been built. The format of the model was simplified and linearized from theoretical results, and the parameters were optimized with experimental data. The friction, although insensitive to velocity, is history dependent, and thus is difficult to model. A constant Coulomb friction was suggested and integrated into the static model to obtain a dynamic model.

Discussion

In the following, comparisons will be given between the McKibben muscles and biological skeletal muscles in terms of static and dynamic properties.

1) Static properties: tension-length-activation relationships

The general shape of the tension-length curve of the actuators is a monotonic increasing function of the length. For the tested nylon shell actuator, the tension reaches zero when the length is shorter than 0.75 L_o (L_o = 14 cm), and becomes very stiff when the length is longer than 1.1 L_o. Between these two points, the stiffness is about constant with a typical value of 23 N/cm (322 N/L_o) at 5 bar, and is approximately proportional to the pressure with some offset. Extrapolating the static model, the maximum tension is 110 N at 1.1 L_o and 5 bar. The integration of the tension within 0.75 to 1.1 L_o is 19 NL_o, which is the maximum output work per mechanical cycle.

In order to calculate the stiffness and tension intensities per unit cross section area and the work per unit volume, we use the external cross section area at maximal shortening as the divider, because this is the maximum cross section area which the actuator should be allowed to occupy in a limb segment. For the nylon shell actuator, the cross section area is 0.95 cm^2 at 0.75 L_o, which yields the stiffness intensity of 340 N/$L_o$cm^2, the maximum tension intensity of 116 N/cm^2, and the work per cycle per unit volume of 0.20 J/cm^3.

The above properties of the other two actuators (fiberglass shell and Bridgestone) are listed in Table 1. The way that the threads form the external braided shell of the actuators influences most differences between the three actuators. The nylon shell actuator consists of a low thread density, middle thickness threads, middle resting braid angle shell, which yields the widest 35% dynamic range, highest work density, and smallest Coulomb friction. The fiberglass shell actuator consists of a high thread density, thin threads, large resting braid angle shell, which yields the largest 15% extensibility, lowest tension and stiffness intensities, and lowest work density. The Bridgestone actuator consists of a high thread density, thick threads, small resting braid angle shell, which yields the narrowest 24% dynamic range, almost no extensibility, and the highest tension and stiffness intensities.

For biological muscles, the tension-length relation can be described by the "active tension" with a trapezoidal shape and the "passive tension" with increasing stiffness when stretched beyond a certain length. There may be a local maximum of the total tension if the increase of passive tension is less than the decrease of active tension to the length.

We now consider a few example parameters of biological muscles. The zero-tension lengths of the active tension are 0.64 and 1.8 L_o (frog striated muscle, Gordon et al. 1966), however, if we define the dynamic range of biological muscles by the non-negative-slope region of the active tension-length curve, then it is within 0.64 to 1.12 L_o. The maximum tension intensity is about 35 N/cm^2 (Guyton 1986, or 30 N/cm^2 from Gordon 1989), this yields the average stiffness intensity of 73 N/$L_o$cm^2, and the work per cycle per unit volume of 0.13 J/cm^3 by numerically integrating the tension-length curve within the dynamic range.

In summary, the biological muscle can be stretched beyond its resting length much longer than the actuators, but usually this is beyond the ordinary physiological oper-

ating region. Also, the biological muscle can shorten a little more than the actuators, this is a major disadvantage of the actuators. On the other hand, the tension intensity of the actuators is much higher than biological muscles, this is a major advantage of the actuators and yields higher work density and stiffness intensity. Finally, to improve the match to biological muscle static properties, passive parallel and serial elastic elements, which exist in biological muscles, can be added into the actuators without difficulty.

2) Dynamic properties: tension-velocity relationships

The tension-velocity relation of the nylon shell actuator, if we do not count the viscosity of the pneumatic circuit, is dominated by a velocity-insensitive Coulomb friction, and the velocity-dependent viscous friction is immeasurable (below 8 L_o/s velocity at least), which yields a very high maximum velocity in theory.

On the other hand, the hyperbolic tension-velocity curve of biological muscles indicates the viscosity decreases when the velocity increases (Hill 1938), and there is no Coulomb friction reported. The typical maximum shortening velocity is 2 L_o/s for slow muscle and 8 L_o/s for fast muscle (Winters 1990) or 20 L_o/s for fast muscle (Gordon 1989).

Obviously the tension-velocity relationship of the actuator is not similar to that of biological muscles. Fortunately, the viscous friction is very small and thus we can add some parallel viscous elements to simulate biological muscles. In addition, although the lubricants used in quasi-static experiments do not significantly reduce the Coulomb friction, there may be some other kinds of lubricant which are more effective.

properties	units	McKibben actuators @ 5 bar			Biological muscles
		Nylon shell	Fiberglass shell	Bridge-stone	
Resting length (L_o)	cm	14.0	20.0	14.7	
Dynamic range	L_o	0.75-1.1	0.85-1.15	0.78-1.02	0.64-1.12
Maximum tension	N	110 @ $1.1L_o$	56 @ $1.15L_o$	260 @ $1.02L_o$	
Stiffness	N/L_o	322	185	1090	
Work per cycle	NL_o	19	8.4	31	
Cross section area	cm^2	0.95 @ $0.75L_o$	0.64 @ $0.85L_o$	1.8 @ $0.78L_o$	
Tension intensity	N/cm^2	116	88	144	35
Stiffness intensity	N/$L_o$cm^2	340	290	606	73
Work density per c.	J/cm^3	0.20	0.13	0.17	0.13
Coulomb friction	N	2.5	5	5	0
Maximum velocity	L_o/s	> 8			2-8 or 20
Avg. power density	W/cm^3	1.1			
Peak power density	W/cm^3	2.65			0.70
Energy efficiency	-	0.32-0.49			0.2-0.25

Table 1: The mechanical properties of the McKibben actuators and biological muscles

Conclusion and future work

The linearized mechanical model of the actuator gave us simple yet accurate descriptions of the actuator behaviors. This can be used in simulation of single or multiple actuator systems for designing consideration.

The static mechanical features of the actuator are very similar to biological muscles, except the dynamic range is narrower and the tension intensity is much higher. Some dynamic features may need to be modified to get even closer, for examples: add some parallel and serial elastic elements in order to fine tune the passive elastic characteristics, use lubricant to reduce the Coulomb friction and add some viscous material to increase the viscous friction in order to fit the tension-velocity relationship.

References

Burke R E, Rudomin P and Zajac F E (1976) The effect of activation history on tension production by individual muscle units. Brain Res. 109: 515-529

Chou C-P and Hannaford B (1992) Dual stable point model of muscle activation and deactivation. Biol. Cybern. 66: 511-523

Chou C-P and Hannaford B (1993) Measurement and modeling of McKibben pneumatic artificial muscles. Submitted to IEEE Trans. Robotics and Automation

Gasser H S and Hill A V (1924) The dynamics of muscular contraction. Proc. R. Soc. B 96: 398-437

Gavrilovic M M and Maric M R (1969) Positional servo-mechanism activated by artificial muscles. Med. & Biol. Engng. 7: 77-82

Gordon A M, Huxley A F and Julian F J (1966) The variation in isometric tension with sarcomere length in vertebrate muscle fibers. J. Physiol. 184: 170-192

Gordon A M (1989) Contraction in skeletal muscle. In: Textbook of physiology, vol 1: excitable cells and neurophysiology, chap 8, 21st edn. Seattle, Washington

Guyton A C (1986) Contraction of skeletal muscle. In: Textbook of medical physiology, chap 11, 7th edn

Hannaford B and Winters J M (1990) Actuator properties and movement control: biological and technological models. In: Multiple muscle systems, Winters J, Woo S (eds). Springer-Verlag, New York

Hill A V (1922) The maximum work and mechanical efficiency of human muscles and their most economical speed. J. Physiol. 56: 19-41

Hill A V (1938) The heat of shortening and the dynamic constants of muscle. Proc. R. Soc. B 126: 136-95

Inoue K (1988) Rubbertuators and applications for robots. Robotics Research: The 4th International Symposium, Bolles R, Roth B (eds). MIT Press, Cambridge, Mass

Levin A and Wyman J (1927) The viscous elastic properties of muscle. Proc. R. Soc. B 101: 218-243

McMahon T A (1984) Fundamental muscle mechanics. In: Muscle, reflexes, and locomotion, chap 1, Princeton University Press, Princeton, New Jersey

Schulte H F Jr (1961) The characteristics of the McKibben artificial muscle. In: The Application of external power in prosthetics and orthotics. National Academy of Sciences-National Research Council, Washington D. C.

Winters J M (1990) Hill-based muscle models: a system engineering perspective. In: Multiple muscle systems, Winters J, Woo S (eds). Springer-Verlag, New York

Zahalak G I (1990) Modeling muscle mechanics (and energetics). In: Multiple muscle systems, Winters J, Woo S (eds). Springer-Verlag, New York